Supporting Information for:

A Bismuth-Halide Double Perovskite with Long Carrier Recombination Lifetime for Photovoltaic Applications

Adam H. Slavney,[†] Te Hu,[§] Aaron M. Lindenberg,[§] and Hemamala I. Karunadasa[*,†]

Departments of [†]Chemistry and [§]Materials Science and Engineering, Stanford University, Stanford, California 94305, United States

[*]*hemamala@stanford.edu*

Experimental section

All manipulations were conducted in air unless otherwise noted. Solvents were of reagent grade or higher purity. All reagents were purchased from commercial vendors and used as received.

Synthesis of $Cs_2AgBiBr_6$ (1)

Solid CsBr (0.426 g, 2.00 mmol) and $BiBr_3$ (0.449 g, 1.00 mmol) were dissolved in 10 mL of 9-M HBr. Solid AgBr (0.188 g, 1.00 mmol) was then added to the solution and the vial was capped and heated to 110 °C. The solution was held at 110 °C for 2 h and then cooled to room temperature. An orange powder precipitated from solution upon sitting at room temperature for ca. 2 h. This solid was filtered on a glass frit and dried under reduced pressure overnight to afford 0.623 g (58.7% yield) of product. Crystals suitable for structure determination were obtained by controlling the cooling rate at 2 °C/hr. Larger crystals (such as the one shown in Figure 1) were obtained by cooling to room temperature at 1 °C/hr. Anal. Calcd. for $Cs_2AgBiBr_6$ (using inductively coupled plasma mass spectrometry): Cs, 25.03%; Bi, 19.68%; Found: Cs, 25.16%; Bi, 19.36%. Analyses for Ag and Br content were not obtained owing to the insolubility of AgBr.

Crystal structure determination

A crystal of **1** was coated with Paratone-*N* oil, mounted on a Kapton® loop, and transferred to a Bruker D8 Venture diffractometer equipped with a Photon 100 CMOS detector. Frames were collected using ω and ψ scans with 18-keV synchrotron radiation (λ = 0.68880 Å). Unit-cell parameters were refined against all data. The crystal did not show significant decay during data collection. Frames were integrated and corrected for Lorentz and polarization effects using SAINT 8.27b and were corrected for absorption effects using SADABS V2012.[1] The space-group assignment was based upon systematic absences, *E*-statistics, agreement factors for equivalent reflections, and successful refinement of the structure. The structure was solved by direct methods, expanded through successive difference Fourier maps using SHELXS-97, and refined against all data using the SHELXTL-2013 software package.[2-4] Weighted *R* factors, R_w, and all goodness-of-fit indicators are based on F^2. Thermal parameters for all atoms were refined anisotropically.

Optical measurements

Absorption data were collected on a Cary 6000i UV-Vis spectrometer equipped with an integrating sphere operating in absorbance mode. A pressed powder sample was mounted on a quartz slide in the center of the sphere such that light was incident normal to the surface. Room-temperature steady-state emission spectra were collected on powders mounted on quartz slides using a Horiba Jobin-Yvon Spex Fluorolog-3 fluorimeter equipped with a 450-W xenon lamp and a thermoelectrically-cooled R928P detector. Incident light was passed through a double-grating monochromator and data were collected using the FluorEssence 2.3.15 software. Low-temperature photoluminescence (PL) was measured using a spectrograph (Acton Research SpectraPro 500i) equipped with a silicon CCD array detector (Hamamatsu). Samples were excited with a 488-nm InGaAs diode laser (Coherent, OBIS). Samples were cooled to liquid helium temperatures using a Janus ST-500 cold-finger cryostat.

Time-correlated single photon counting (TCSPC) measurement

Measurement was performed using a TCSPC system (TimeHarp 260 PICO, PicoQuant). Powder and single-crystal samples were excited using a 500-fs fiber laser with the frequency doubled from the

fundamental wavelength of 1030 nm to 515 nm. The repetition rate was decreased from 1.28 MHz to 426.7 kHz using an acousto-optic modulator (R35085-50-5-I-HGM-W, Gooch & Housego). PL was detected using a hybrid photomultiplier detector assembly (PMA Hybrid 06, PicoQuant). The detection wavelength was selected using 641/75 nm bandpass filters (Semrock, Inc.), and the excitation fluence was controlled using reflective neutral density filters (NDK01, Thorlabs, Inc.). The response function of the system has a full width at half maximum (FWHM) of ca. 120 ps. Data were collected in 0.8-ns increments. Fluence was varied between 30 nJ/cm^2 and 170 nJ/cm^2 for these measurements.

TCSPC fitting

TCSPC data were fit using OriginPro 8. Time points were shifted such that t = 0 corresponded to the point of maximum intensity. The background signal was subtracted and the data were normalized on the interval [0,1]. The background was determined by taking the mean of the 13 data points immediately prior to t = 0. The background varied between 1–4% and 0.1–0.7% of the maximum PL intensity for single-crystal and powder data sets, respectively. Fitting was only performed out to 1800 ns as later time points begin to merge with the detector noise. In order to prevent the large values at early time points from unduly influencing the fit a statistical weighting function, $w(y_i)$, was applied. The "best fit" was found by minimizing the weighted sum of least squares:

$$\sum_i^N w(y_i) * \left(y_i - y_{i_{fit}}\right)^2 = \sum_i^N \frac{\left(y_i - y_{i_{fit}}\right)^2}{y_i}$$

Fits were performed via an iterative process using the following general equation:

$$I(t) = \sum_i I_i e^{-t/\tau_i}$$

The later part of the data (t > 400 ns) was initially fit with a single exponential. Earlier time points were gradually included in the fit until the fit diverged from the data at which point a new exponential term was added. The addition of the new term was evaluated by comparing the χ^2 statistic of the fits with and without the new term. If χ^2 was reduced the new term was accepted and fitting continued. In all cases three exponential terms were found to best describe the data.

Estimating the fraction of excited carriers that relax via the long-lived recombination pathway

The integral out to infinite time of an exponential function has an analytical solution:

$$\int_0^\infty I_i e^{(-t/\tau_i)}\, dt = I_i \times \tau_i$$

Using the fit parameters for the long-lifetime PL decay process ($E_{fit} = I_3 \times \tau_3$) and numerical integration of the entire PL trace (E_{tot}), we can estimate the fraction of excited carriers that relax via the long-lived recombination pathway in single-crystal and powder samples as (%Long):

$$\frac{E_{fit,xtal}}{E_{tot,xtal}} * 100 = \%Long_{xtal} = 85\ \% \qquad \frac{E_{fit,powder}}{E_{tot,powder}} * 100 = \%Long_{powder} = 80\%$$

The ratio of the single-crystal and powder percentages:

$$\frac{\%Long_{powder}}{\%Long_{xtal}} = 0.94$$

implies that the additional defects and surface sites present in the powder sample only reduce the fraction of long-lived carriers by 6% compared to the single crystal. Numerical integration of the entire PL trace (E_{tot}) was performed in MATLAB using a trapezoidal integration algorithm (trapz).

Other physical measurements

Powder x-ray diffraction (PXRD) measurements were performed on a PANalytical X'Pert powder diffractometer with a Cu anode ($K\alpha_1$ = 1.54060 Å, $K\alpha_2$ = 1.54443 Å, $K\alpha_2/K\alpha_1$ = 0.50000), a programmable divergence slit with a nickel filter, and a PIXcel^{1D} detector. The instrument was operated in a Bragg-Brentano geometry with a step size of 0.02° (2θ). The simulated PXRD pattern was calculated using the crystallographic information file (CIF) from the single-crystal X-ray diffraction experiment. Thermogravimetric and differential thermal analyses were performed with a Netzsch TG 209 F1 Libra Thermo-Microbalance with alumina pans at a heating rate of 5 °C/min, using 30-mg samples. Photoelectron spectroscopy in air (PESA) measurements were performed using a Riken AC-2 photoelectron spectrometer on a pressed pellet of **1**. Scanning electron micrographs of powder samples were taken using a FEI XL30 Sirion SEM. Raman spectroscopy was performed using a Renishaw RM1000 Raman microscope. The sample was excited at 514 nm using an Ar-ion laser with a power of 2.5 mW. Inductively coupled plasma mass spectrometry (ICP-MS) measurements to determine elemental composition were conducted in 5% nitric acid solutions using a Thermo XSeries II ICP-Mass Spectrometer.

Stability studies

Freshly prepared powder samples of **1** were placed on clean glass slides for this experiment. For the humidity study a sample was placed on a platform inside a Teflon-capped glass jar. The bottom of the jar was filled with saturated $Mg(NO_3)_2$ solution so that the relative humidity above the surface of the liquid was maintained at 55%.[5] The outside of the jar was covered with electrical tape to minimize light exposure. For the light stability study a sample was placed in a custom built chamber and irradiated with a broad spectrum halogen lamp (intensity = 0.75 Suns, calibrated with a photodiode). The lamp irradiated the sample through the glass of the chamber so only wavelengths greater than 280 nm reached the sample. A thermocouple was placed within the chamber to monitor the sample temperature. The temperature varied from 45 °C to 65 °C over the course of the experiment with an average temperature of ca. 50 °C. The sample was kept under flowing dry nitrogen gas. Both samples were checked by eye daily and monitored by PXRD at regular intervals. All samples were briefly exposed to ambient conditions during PXRD measurements.

Table S1. Crystallographic data[a] for $Cs_2AgBiBr_6$ (**1**)

Empirical Formula	$Cs_2AgBiBr_6$
Formula Weight, g·mol^{-1}	1062.07
Temperature, K	300(0)
Crystal System	Cubic
Space group	*Fm*-3*m*
a, Å	11.2499(4)
b, Å	11.2499(4)
c, Å	11.2499(4)
α, β, γ °	90
Volume, Å^3	1423.79(9)
Z	4
Density (calculated), g·cm^{-3}	4.955
Absorption coefficient, mm^{-1}	32.683
F(000)	1800
Crystal size, mm^3	0.15 × 0.10 × 0.05
θ range, °	6.078 to 54.54
Index ranges	$-14 \le h \le 14$ $-14 \le k \le 14$ $-14 \le l \le 14$
Reflections collected/unique	6134/122
Completeness to θ_{max}, %	100
Max. and min. transmission	0.292, 0.086
Data/restraints/parameters	122/0/8
Goodness-of-fit on F^2	1.200
Final *R* indices [$I > 2\sigma(I)$][b]	$R_1 = 0.0108$ w$R_2 = 0.0230$
R indices (all data)[b]	$R_1 = 0.0108$ w$R_2 = 0.0230$
Largest diff. peak and hole, e·Å^{-3}	0.264, –0.395

[a]Obtained with 18-keV synchrotron (λ = 0.68880 Å) radiation.
[b]$R_1 = \Sigma||F_o| - |F_c||/\Sigma|F_o|$, w$R_2 = [\Sigma w(F_o^2 - F_c^2)^2/\Sigma(F_o^2)^2]^{1/2}$

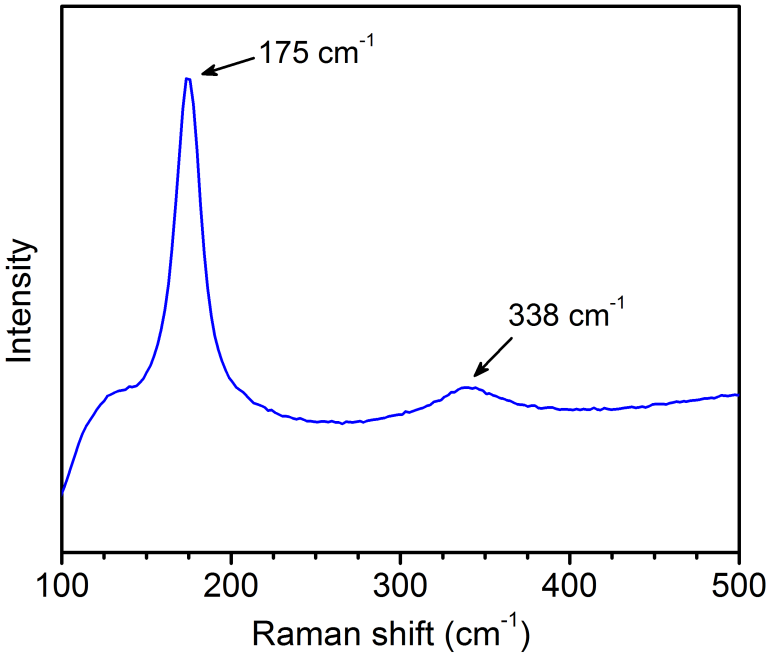

Figure S1. Raman spectrum of **1**.

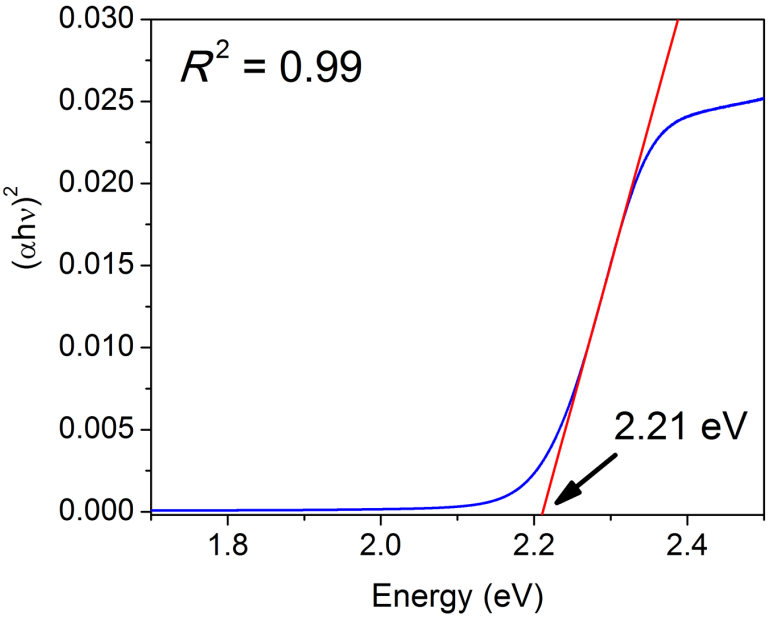

Figure S2. Tauc plot of the absorbance data for a direct allowed transition in **1**. Fits to the linear portion of the plot give the direct bandgap as 2.21 eV.

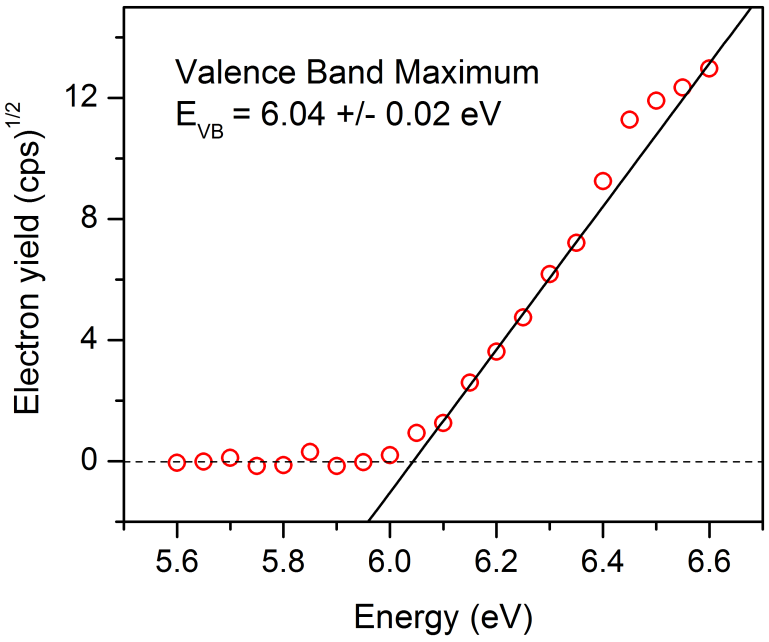

Figure S3. Valence band maximum determination using photoelectron spectroscopy in air (PESA) on a pressed pellet of **1**.

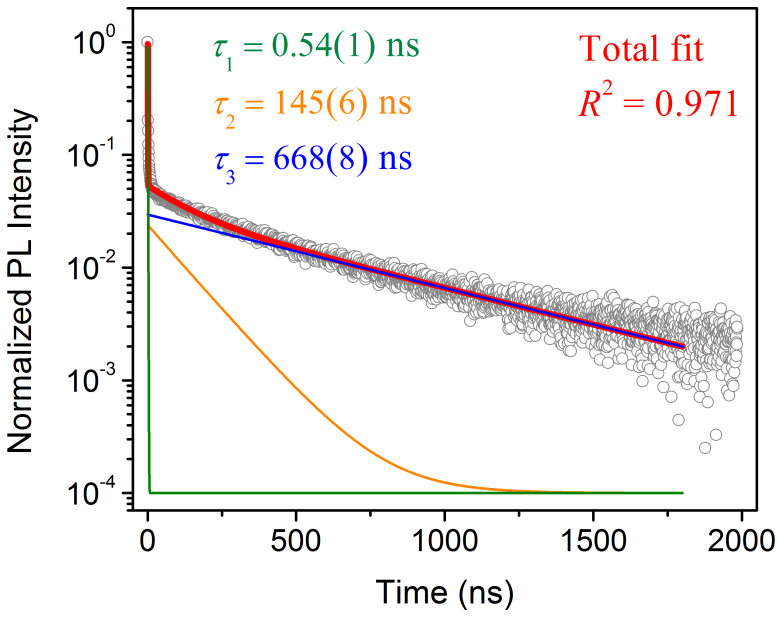

Figure S4. Full fit of the single-crystal time-resolved photoluminescence data.

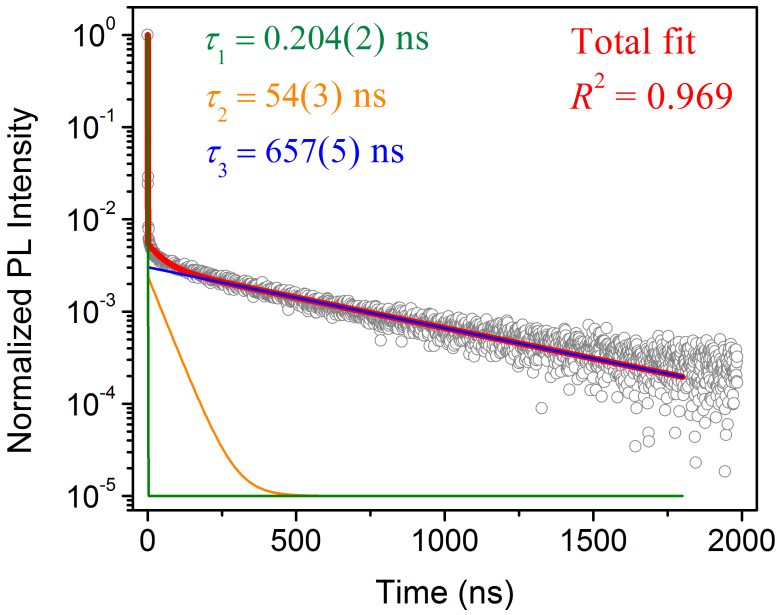

Figure S5. Full fit of the powder time-resolved photoluminescence data.

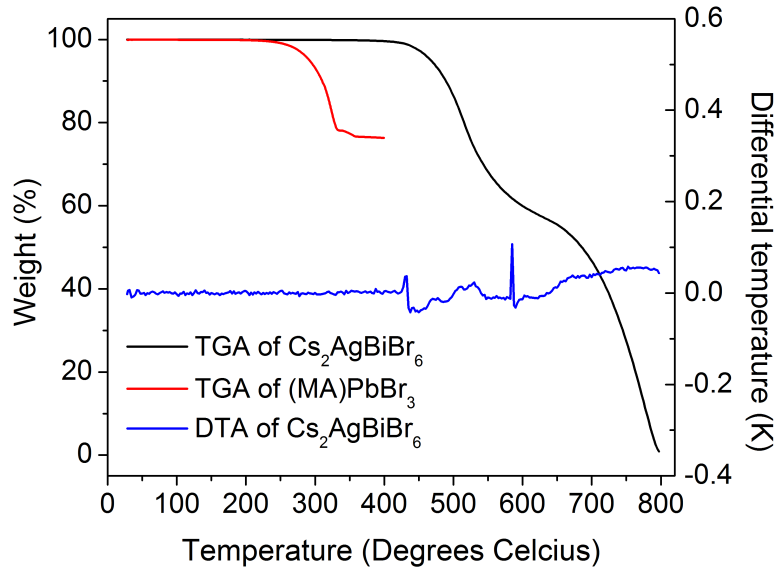

Figure S6. Thermogravimetric analyses of **1** and $(MA)PbBr_3$ at a scan rate of 5 °C/min and 1 °C/min, respectively. Solid $(MA)PbBr_3$ shows an initial mass loss at 176 °C. Solid **1** shows an initial mass loss at 430 °C. DTA of **1** shows no phase changes until the mass loss onset.

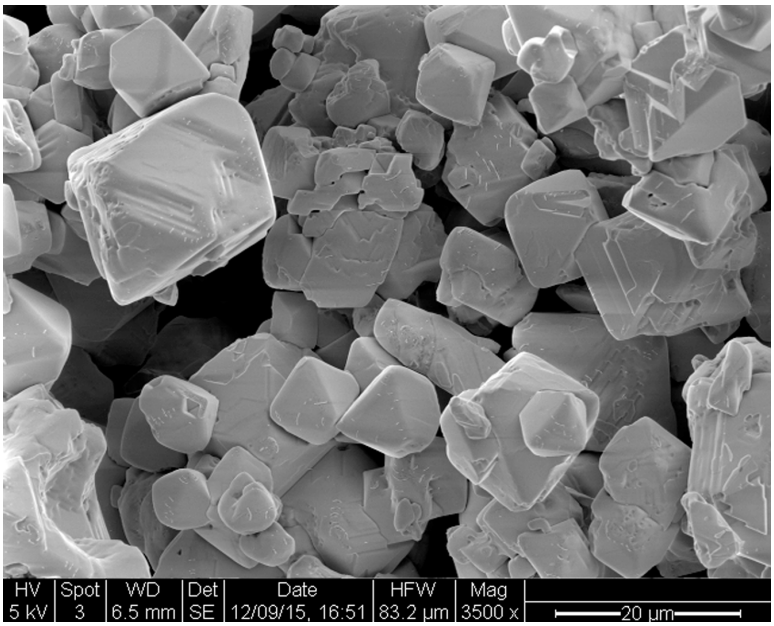

Figure S7. Electron micrograph of **1** powder used for TRPL measurements. The sample has a large distribution of particle sizes but the majority are between 1–20 µm.

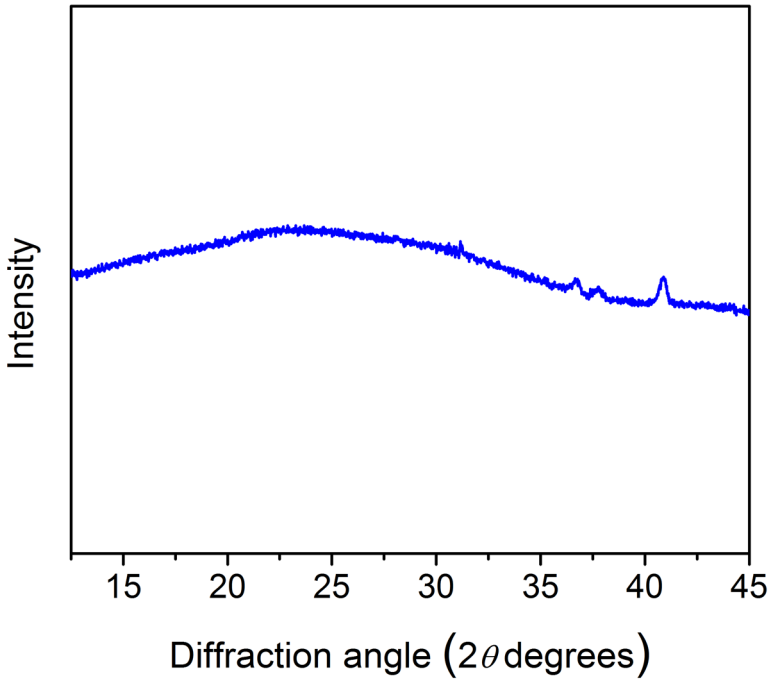

Figure S8. Powder XRD of the sample stage. Peaks shown here correspond to reflections marked by asterisks in Figure 3A.

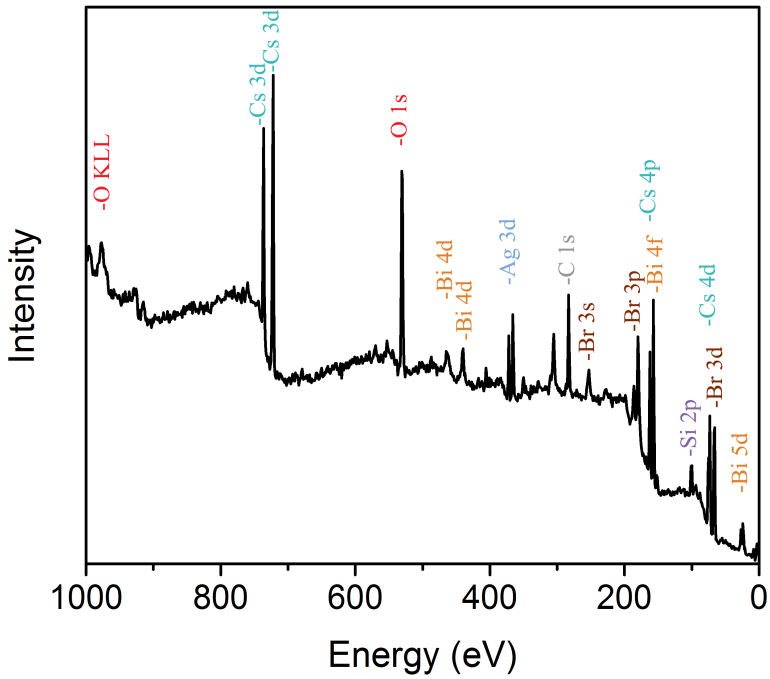

Figure S9. X-ray photoelectron spectroscopy of a single crystal of **1**. Signals from O, C, and Si originate from the adhesive tape used to hold the sample.

References

(1) Bruker AXS Inc.: Madison, Wisconsin, 2007.
(2) Sheldrick, G. M. *Acta. Cryst. Sect. A* **2008**, *64*, 112.
(3) Muller, P., Herbst-Irmer, R., Spek, A. L., Schneider, T. R., Sawaya, M. R. *Crystal Structure Refinement: A Crystallographer's Guide to SHELXL*; Oxford University Press: New York, 2006.
(4) Sheldrick, G. M. Göttingen, 1997.
(5) Wexler, A.; Hasegawa, S. *J. Res. Natl. Bur. Stand.* **1954**, *53*, 19.